Dependence of tropical cyclone weakening rate in response to an imposed moderate environmental vertical wind shear on the warm-core strength and height of the initial vortex

Qi Gao[a,b] and Yuqing Wang[c]

[a]Department of Atmospheric and Ocean Sciences, Institute of Atmospheric Sciences, Fudan University, Shanghai, China

[b]State Key Laboratory of Severe Weather, Chinese Academy of Meteorological Sciences, China Meteorological Administration, Beijing, China

[c]International Pacific Research Center and Department of Atmospheric Sciences, School of Ocean and Earth Science and Technology, University of Hawaii at Manoa, Honolulu, HI, USA

December 8, 2023 (submitted)

January 31, 2024 (first revision)

February 29, 2024 (second revision)

Dateline

Key Points:

- The TC weakening rate in response to an imposed moderate environmental VWS is proportional to the strength and height of the TC warm core.
- The warm-core weakening induced by upper-level ventilation is the primary factor to the early TC weakening induced by the imposed VWS.
- The boundary-layer ventilation shows no relationship with the early weakening rate of the TC in response to the imposed moderate VWS.

Submitted to ***Geophysical Research Letters***

Corresponding author: Yuqing Wang, yuqing@hawaii.edu

Abstract

This study investigated the dependence of the early tropical cyclone (TC) weakening rate in response to an imposed moderate environmental vertical wind shear (VWS) on the warm-core strength and height of the TC vortex using idealized numerical simulations. Results show that the weakening of the warm core by upper-level ventilation is the primary factor leading to the early TC weakening in response to an imposed environmental VWS. The upper-level ventilation is dominated by eddy radial advection of the warm-core air. The TC weakening rate is roughly proportional to the warm-core strength and height of the initial TC vortex. The boundary-layer ventilation shows no relationship with the early weakening rate of the TC in response to an imposed moderate VWS. The findings suggest that some previous diverse results regarding the TC weakening in environmental VWS could be partly due to the different warm-core strengths and heights of the initial TC vortex.

Plain language summary

The warm core is a basic structural feature of a tropical cyclone (TC), and TC intensity is closely related to the warm-core strength and height. This study investigated the dependence of the initial TC weakening rate in response to an imposed moderate environmental vertical wind shear (VWS) on the strength and height of the TC vortex during the TC intensifying period using idealized numerical simulations. It is found that the weakening of the warm core is the primary factor leading to the early weakening of the TC, and the TC weakening rate is roughly proportional to the warm-core strength and height of the TC vortex. It is also found that the boundary-layer ventilation associated with VWS-induced convective downdrafts show no relationship with the early weakening rate of the TC in response to an imposed moderate VWS. The findings of this study can help explain why some TCs can continuously develop under the influence of moderate environmental VWS while some others cannot, which are partly due to the different warm-core strengths and heights of the initial TC vortex.

1. Introduction

Environmental vertical wind shear (VWS) is an essential dynamical factor that affects the tropical cyclone (TC) structure and intensity change, which has been extensively studied in the literature (e.g., Braun & Wu, 2007; Gray, 1968; Gu et al., 2015, 2018, 2019; Tang & Emanuel, 2012; Wang & Holland, 1996; Wang et al., 2015; Xu & Wang, 2013; Zeng et al., 2010). Previous studies identified several ventilation effects associated with the impact of environmental VWS on TC intensity change, including the so-called “upper-level ventilation”, “mid-level ventilation”, “low-level ventilation” (Frank & Ritchie, 2001; Gray, 1968; Riemer et al., 2010; Tang & Emanuel, 2010, 2012), and also “radial ventilation” and “downdraft ventilation” as recently presented by Alland et al. (2021a, 2021b).

Zehr (1992) found that if the environmental VWS between 200–850 hPa was greater than 10 m s^{-1}, TCs in the western North Pacific generally did not form or develop. However, Nguyen & Molinari (2012) showed that the ambient southwesterly VWS of Hurricane Irene (1999) increased from 6–7 m s^{-1} to 10–13 m s^{-1} during rapid intensification. Therefore, although large VWS is known to be detrimental to TC genesis and often leads to TC weakening, large uncertainty on the TC intensity change remains for TCs embedded in a moderate environmental VWS, namely around 10 m s^{-1} (see also Bhatia & Nolan, 2013; Chen et al., 2021; Hendricks et al., 2010; Molinari et al., 2006; Reasor & Eastin, 2012; Ryglicki et al., 2019).

We conjecture that the uncertainty in the effect of moderate environmental VWS may arise from the dominant role of different ventilation pathways mentioned above. The mid- and upper-level ventilations suggest the “top-down” pathway of TC weakening. Namely, the warm-core structure of the TC weakens from the top down in response to an imposed environmental VWS (Alland et al., 2021b; Frank & Ritchie, 2001; Fu et al., 2019; Gray, 1968; Tang & Emanuel, 2010). The low-level ventilation hypothesis suggests the “bottom-up” weakening of the TC, namely the TC weakening is triggered by the decrease of eyewall entropy in the boundary layer (Alland et al., 2021a; Gu et al., 2015; Riemer et al., 2010). Fu et al. (2019) pointed out that the ventilation of the upper-level warm core played the most important role in TC weakening in response to an imposed moderate upper-level and lower-level VWS, respectively, during the mature stage of the TC. Their results supported the "top-down" pathway of TC weakening, while results of Riemer et al. (2010) seemed to support the dominant role of the low-level ventilation in TC weakening by adding the moderate to strong deep-layer VWS to the TC during its intensifying stage. Therefore, the way by which an imposed moderate environmental VWS affects the TC intensity change, particularly the predominant pathway of initial TC weakening process, has not been fully understood.

The "upper-level ventilation" pathway is closely related to the weakening of the warm core. A question arises as to how the TC weakening rate in response to the imposed moderate environmental VWS depends on the intensity and thus the warm-core strength and height of the initial TC vortex. Previous studies have conducted numerical experiments using either initially weak or strong TCs, and thus with different warm-core strengths and heights (Fu et al., 2019; Gu et al., 2015; Onderlinde & Nolan, 2017; Reasor et al., 2013). Riemer et al. (2010) found in their idealized simulation that for mature storms the moderate to strong VWS might produce persistent vortex-scale downdrafts, flushing the boundary layer and leading to the TC weakening. However, Nguyen et al. (2019) focused on relatively weak TCs and found that enhanced surface enthalpy flux produced by high surface winds of intensifying TCs allowed downdraft-modified boundary layer air to recover effectively and quickly. Riemer & Montgomery (2011) found that stronger TCs are more resilient to radial ventilation. These studies seem to suggest that weak TCs are less resistant to moderate to strong VWS than strong TCs. However, many other studies have shown that weaker TC vortices can intensify rapidly in moderate environmental VWS after a period of adjustment (Molinari et al., 2006; Rios-Berrios et al., 2016; Rios-Berrios, 2020).

Most above studies have focused only on one category of weak or strong sheared TCs. However, few studies have focused on TCs at different intensifying stages under the influence of an imposed moderate environmental VWS. Finocchio & Rios-Berrios (2021) described a set of idealized simulations using the point-downscaling method in which VWS increases from 3 to 15 m s^{-1} at different stages of an intensifying TC. They found that all experiments exhibited hindered TC intensification, and TCs exposed to increasing shear during or just after rapid intensification tended to weaken the most. However, their study focused on strong environmental VWS, which increases with time to reach 15 m s^{-1}. As mentioned above, the diverse intensity changes have been reported in previous studies for TCs embedded in moderate environmental VWS.

In a recent study, Gao & Wang (2023) found a strong dependence of TC weakening in response to an imposed moderate VWS on the stage of an intensifying TC. Since the different stages of the intensifying TC correspond to different warm-core strengths and heights of the TC, they hypothesized that the TC intensity change rate in response to an imposed moderate VWS might depend on the warm-core strength and height of the initial TC vortex, which was defined as the maximum potential temperature (θ) anomaly over the TC center relative to the TC environment (Xi et al., 2021). The environmental θ at a certain level was defined as the mean θ of the outermost grids in four directions in the outermost domain. Because Gao & Wang (2023) focused on how the asymmetric structure of the initial TC vortex affects the TC intensity change in response to an imposed moderate VWS, they did not examine the detailed physical processes. This study can be considered as an extension of Gao & Wang (2023) with the focus on the dependence of the initial weakening rate of an intensifying TC on the warm-core strength and height in response to an imposed moderate VWS on an *f*-plane using idealized numerical experiments performed in Gao & Wang (2023).

2. Model and experimental design

The three-dimensional, compressible, nonhydrostatic, full-physics Weather Research and Forecasting (WRF) model version 4.2.2 (Skamarock et al., 2008) was used to conduct a series of numerical experiments as in Gao and Wang (2023). All numerical experiments were conducted on an *f*-plane at 15°N over the ocean with a uniform sea surface temperature of 28.5°C. The initial unperturbed sounding of the model atmosphere was the moist-tropical sounding documented in Dunion (2011). The initial TC vortex in the control experiment was axisymmetric and in gradient and thermal wind balance as in Rotunno and Emanuel (1987) with a maximum tangential wind speed of 18 m s^{-1} near the surface at a radius of 90 km. The other model settings and experimental design are the same as those described in Gao and Wang (2023) and thus are not repeated here. The vertical profile of the environmental zonal winds is showed in Figure 1a (inset vignette). Only results from four VWS experiments with an initially axisymmetric TC vortex in Gao and Wang (2023) are used in this study. Namely, in these experiments, the moderate environmental VWS was imposed onto an initially axisymmetric vortex after 24 (SHE24_AXI), 48 (SHE48_AXI), 72 (SHE72_AXI), and 96 h (SHE96_AXI) of the simulation during the TC intensifying period in a quiescent environment experiment (CTRL), respectively.

3. Results

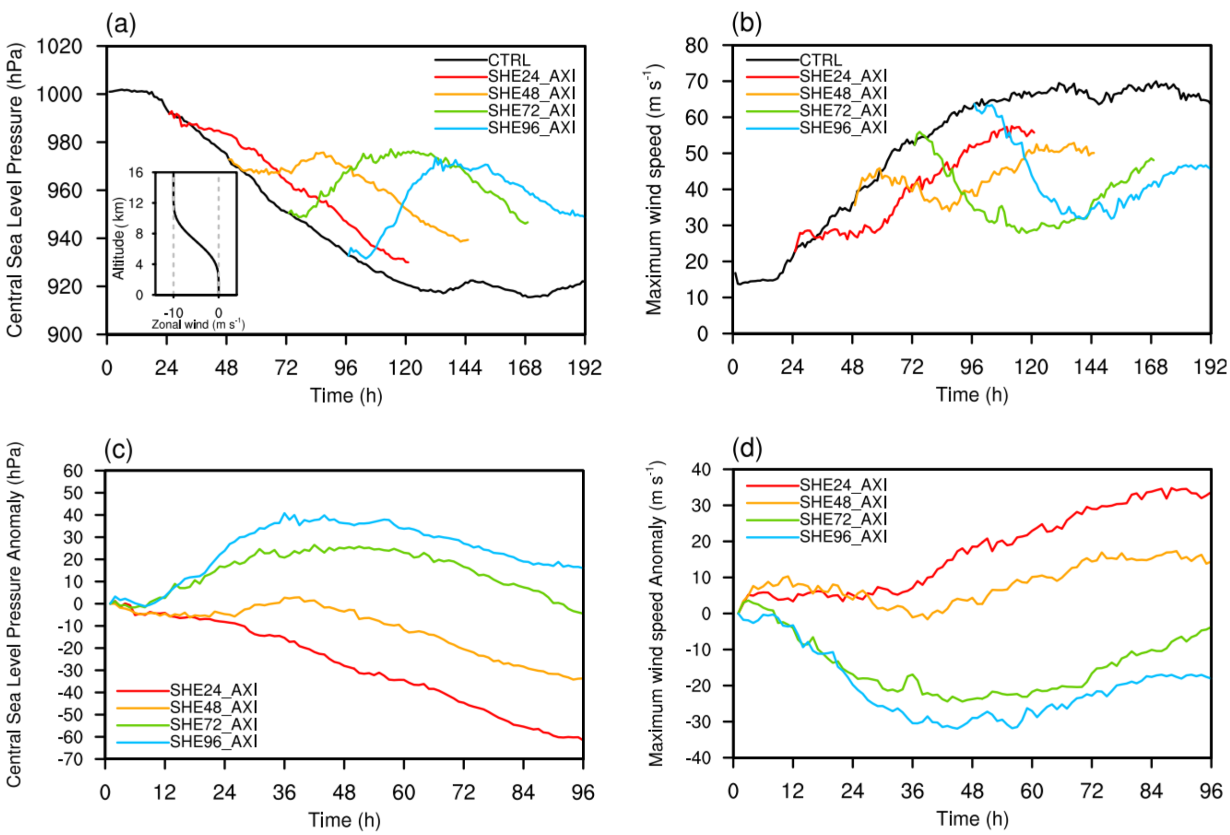

Figure 1. Time evolutions of (a) the simulated central sea level pressure (hPa), (b) the maximum near-surface wind speed (m s^{-1}) in CTRL (black) and in all easterly VWS experiments (colored), and (c, d) the differences from their corresponding values at the initial time in CTRL. The inset vignette indicates the vertical profile of the environmental zonal wind. The colors represent the VWS experiments as given in each panel.

Figures 1a and 1b show the time evolutions of the TC intensity in terms of the central sea level pressure and the maximum azimuthally averaged total wind speed at the lowest model level (30 m above sea level) in CTRL (black) and four VWS experiments initialized with the axisymmetric TC vortices after 24, 48, 72, and 96 h of the simulation in CTRL (colored), respectively. We can see that the TC experienced a reduced intensification rate in the early intensifying stage (SHE24_AXI and SHE48_AXI), while the TC experienced obvious weakening when the moderate VWS was imposed onto the TC vortices at the later intensifying stage (SHE72_AXI and SHE96_AXI). The TC weakening rate increases roughly with the increasing initial TC intensity at the time when the VWS is added (Figures 1c and 1d).

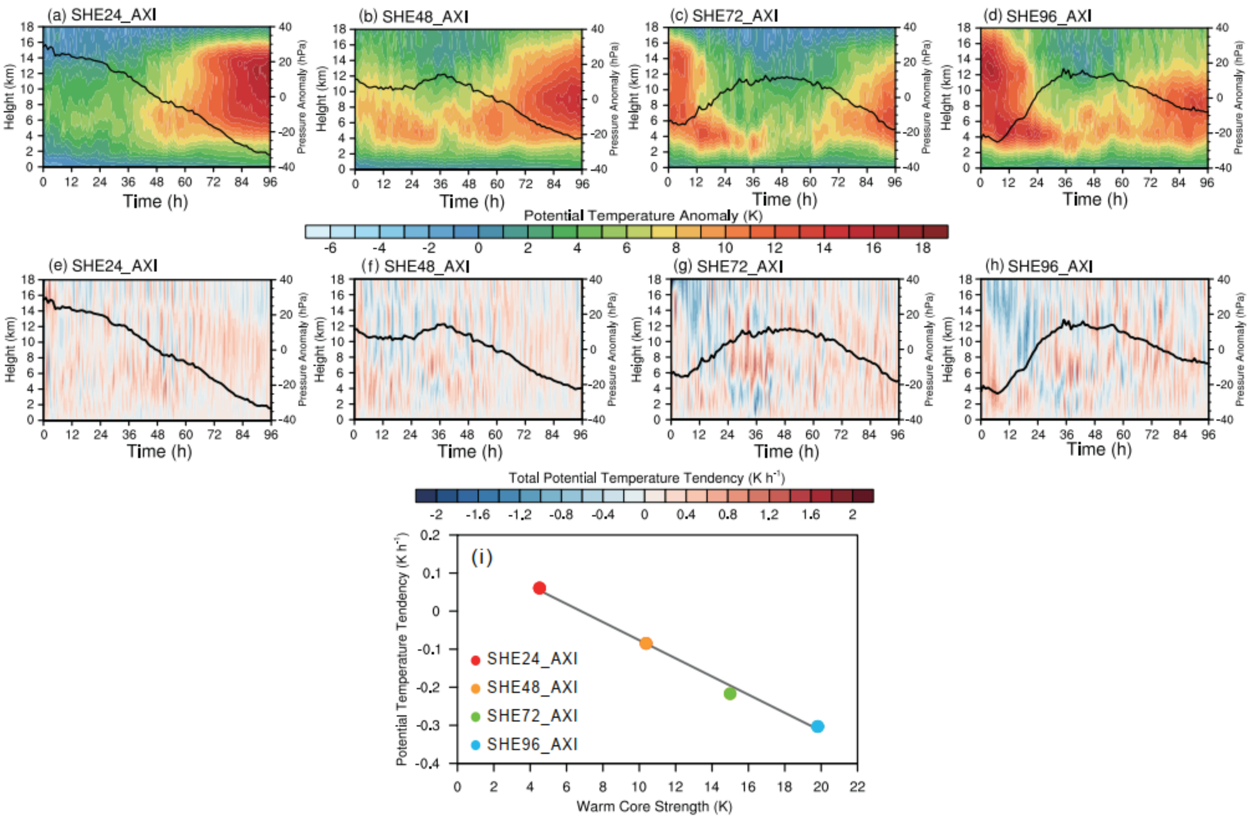

Figure 2. (a-d) Time-height cross section of the θ anomaly (shading; K) and (e-h) the θ tendency (shading; K h^{-1}) averaged within a radius of 50 km from the surface TC center obtained from the model output at 6-min intervals during the simulations, along with the time evolution of the central sea level pressure anomaly of the TC in each VWS experiment (black solid, hPa, right axis). (i) The scatter plots (dots) of the warm-core strength (K) versus the θ tendency (K h^{-1}) averaged between 10–16-km heights during 0–24 h in VWS experiments, the gray line shows the linear fitting.

The initial vortices at the time when the moderate environmental VWS was introduced correspond to different warm-core strengths and heights at different intensifying stages of the TC (Figures 2a-d). The initial TC vortex in SHE24_AXI had a very weak and lower upper-level warm core (Figure 2a), with a weak θ anomaly maximized near 8 km altitude. The warm core intensified with positive θ tendency (Figure 2e) even after the VWS was introduced, indicating that the VWS had little effect on the TC intensification at the early stage of an intensifying TC. The initial TC vortex in SHE48_AXI had a weak warm core centered at the height of 8 km (Figure 2b). The warm core weakened slightly after the VWS was introduced (Figure 2f), which is consistent with the slowed intensification followed by a slight weakening of the TC during the first 36 h in SHE48_AXI. However, the initial TC vortices in SHE72_AXI and SHE96_AXI had stronger and higher (near the height of 15-16 km) upper-level warm cores (Figures 2c-d). The strong and high warm core weakened significantly in response to the imposed moderate VWS. The θ tendency showed negative values from top down as the TC weakened (Figures 2g-h). This strongly suggests that the weakening of the warm core is the important factor reflecting to the early weakening rate of the TC. As we can see from Figure 2i, which shows the θ tendency averaged between 10–16 km heights during 0–24 h and the warm core strength in each VWS experiment, the θ tendency is almost linearly proportional to the warm-core strength of the initial TC vortex.

To understand the warm-core weakening processes of the simulated TCs in the shear experiments, we performed a budget analysis for the azimuthal mean potential temperature ($\bar{\theta}$) during the warm-core weakening stage in SHE72_AXI as an example. The budget equation can be given below (Stern & Zhang, 2013):

$$\Delta\bar{\theta} = (TADV + HEAT + PBL + HDIF)\Delta t \quad (1)$$

where $\Delta\bar{\theta}$ is the actual change of $\bar{\theta}$ over a given period of Δt; TADV, HEAT, PBL, HDIF are the tendencies of $\bar{\theta}$ contributed by, respectively, both horizontal and vertical advection of $\bar{\theta}$, the azimuthal mean diabatic heating, boundary layer turbulent mixing, and subgrid-scale horizontal diffusion. Since HDIF is quite small, it is not considered in our following discussion. All terms on the right-hand side of Eq. (1) were directly obtained from the model output at 6 min intervals during the model simulations. Following previous studies (Stern & Zhang, 2013, Wang et al., 2019, Liu et al., 2021), we further decomposed the total advection term (TADV) into the horizontal and vertical advection and azimuthal mean and eddy advection components. Namely, we have $TADV = RADVM + VADVM + RADVE + VADVE$. Terms on the right-hand side represent the mean radial advection, mean vertical advection, eddy radial advection, and eddy vertical advection, respectively, defined below:

$$
\begin{aligned}
RADVM &= -\bar{u}\frac{\partial\bar{\theta}}{\partial r} \\
VADVM &= -\bar{w}\frac{\partial\bar{\theta}}{\partial z} \\
RADVE &= -\frac{\partial}{\partial r}\overline{(u'\theta')} - \frac{\overline{(u'\theta')}}{r} \\
VADVE &= -\frac{\partial}{\partial z}\overline{(w'\theta')}
\end{aligned} \tag{2}
$$

where u and w are the radial and vertical velocities, respectively, r and z are radius and height. In Eq. (2), the overbar denotes the azimuthal mean, and the prime denotes the deviation from the corresponding azimuthal mean. The variables u, w, and θ are also output at 6-min intervals. The vortex center at the lowest model level was used to calculate the azimuthal mean.

Figure 3 shows the $\bar{\theta}$ budget results for the 12-h period from 6 to 18 h of the simulation in SHE72_AXI during which the TC was in its early weakening stage (Figure 1). The actual $\bar{\theta}$ change is mostly positive below 6 km height and negative above (Figure 3a). The large negative change in the layer between 14 and 16 km heights indicates the ventilation of $\bar{\theta}$ in the upper troposphere, suggesting a top-down weakening of the warm core of the simulated TC in response to the imposed VWS. The budgeted $\bar{\theta}$ change is generally consistent with the actual $\bar{\theta}$ change (Figure 3b). Although some unavoidable discrepancies between the actual and the budgeted $\bar{\theta}$ changes exist mainly due to the ignored HDIF, the decomposition and interpolation from the Cartesian coordinates to the cylindrical coordinates, the discrepancies are generally small. The large negative $\bar{\theta}$ change inside a radius of 30 km in the upper troposphere was mainly contributed by advection terms (Figures 3e–3h). Since the mean vertical advection (Figure 3f) is nearly balanced by the contribution of diabatic heating (Figure 3d) in the eyewall region, the azimuthal mean and eddy radial advections dominated the negative $\bar{\theta}$ change in the upper troposphere (Figures 3e and 3g) and thus the warm-core ventilation. The mean radial advection is smaller than the eddy horizontal advection, suggesting that the radial eddy advection was key to the upper-level warm-core ventilation. This is consistent with the result of Frank & Ritchie (2001). Note that the low-level ventilation in the boundary layer will be explained in detail later.

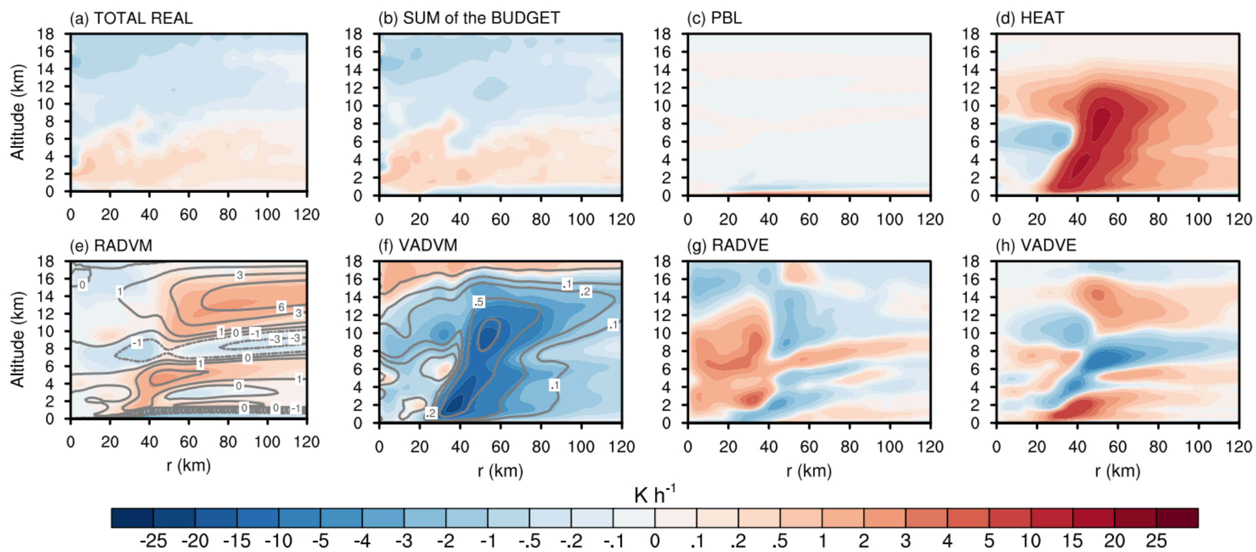

Figure 3. Radial-height cross sections of $\bar{\theta}$ budget terms (K h^{-1}; shading). (a) The actual 12-h change of $\bar{\theta}$, (b) the sum of the right-hand side of Eq. (1); terms on the right-hand side contributed by (c) PBL; (d) diabatic heating (HEAT); (e) the azimuthal mean radial advection (RADVM); (f) the azimuthal mean vertical advection (VADVM); (g) eddy radial advection (RADVE); (h) eddy vertical advection (VADVE), based on the model output at 6-min intervals from 6 to 18 h of the simulation in SHE72_AXI. Contours in (e) and (f) are the radial wind speed and vertical motion, respectively (m s^{-1}, solid is positive and dashed is negative).

To understand how the high θ air within the upper-level warm core is transported outward, leading to the weakening of the warm core, we tracked the air particles using an advection correction trajectory algorithm following Miller & Zhang (2019), Liu et al. (2022), and Dai et al. (2023). Since the warm core in SHE72_AXI was centered at about 15–16 km height, we chose 16 km and 13 km as examples to show how the warm-core particles were transported outward and the surrounding particles were transported inward during the early TC weakening (Figures 4a-b, e-f). We also calculated the change of θ_e in the warm core during this stage. We selected 375 particles within the radius of 50 km from the TC center at the initial heights of 16 and 13 km and at the time of 6 h (14 h) after the VWS was introduced as the initial tracking warm-core particles and tracked them forward (backward) for 8 h. We calculated the averaged θ_e of the particles at the time of 6-h based on the forward trajectory, which were transported outward from the region within the 50-km radius, which corresponded to air particles of the warm core. We also calculated the averaged θ_e of the particles at the time of 14 h based on the backward trajectory, which was transported inward from outside the 50-km radius and replaced the air in the original warm core from the outer core and weakened the warm core during this period. Combining the results of backward and forward trajectories, we found that the θ_e decreased by 7.28 K during the 8 hours at the 16-km height and by 1.5 K at the 13-km height due to the radial export of warm parcels in SHE72_AXI. Since the warm core centered at around the 8-km height in SHE24_AXI, we also conducted the same trajectory analysis for SHE24_AXI to make a comparison with SHE72_AXI but at the heights of 10 and 8 km (Figures 4c-d, g-h). Results show that θ_e increased by 0.82 K during the 8 hours at the 10-km height and by 0.83 K at the 8-km height instead of weakening like in SHE72_AXI, which is consistent with the intensification of the TC during this period. To further illustrate the VWS effect, we also show the corresponding results with no-shear environment in CTRL in supplementary Figures S1 and S2. We can see that there are much less particles that are transported outward from the warm core and the θ_e in the warm core increased, especially at the height of 16 km in SHE72_AXI, during the 8 h. Therefore, the comparisons between these results clearly demonstrate that the VWS substantially enhanced the radial ventilation in the upper levels compared to the no-shear environment.

As we can see from Figure 4, the stronger environmental flow at higher levels led to stronger eddy outflow, which transported more warm particles outward, leading to the stronger upper-level ventilation for the TC with a stronger and higher warm core (Figures 2a-d) and thus weakening of the TC as inferred from the hydrostatic relationship (Durden, 2013; Ohno et al., 2016; Shi & Chen, 2021). The stronger initial TCs (SHE72_AXI and SHE96_AXI) with higher-level warm core are subject to stronger outflow induced by the imposed VWS and thus larger weakening rate of the warm core and the TC (Figure 3 and Figure S5), while the weaker initial TCs (SHE24_AXI and SHE48_AXI) with weaker and lower warm core are subject to relatively weaker eddy outflow and thus weaker ventilation of the warm core and less weakening of the TC (Figures S3-S4). In the very early intensifying stage (SHE24_AXI), the warm core of the TC is too weak and too low to be ventilated, and thus the TC is little affected by the imposed moderate VWS (Figure S3). The TC in SHE96_AXI weakened slightly more rapidly than that in SHE72_AXI mainly because the upper-level warm core and thus the upper-level ventilation is stronger in the former than in the latter

(Figure S5). Therefore, the stronger the initial vortex with a stronger and higher warm core, the more the initial weakening of the TC in response to an imposed moderate VWS.

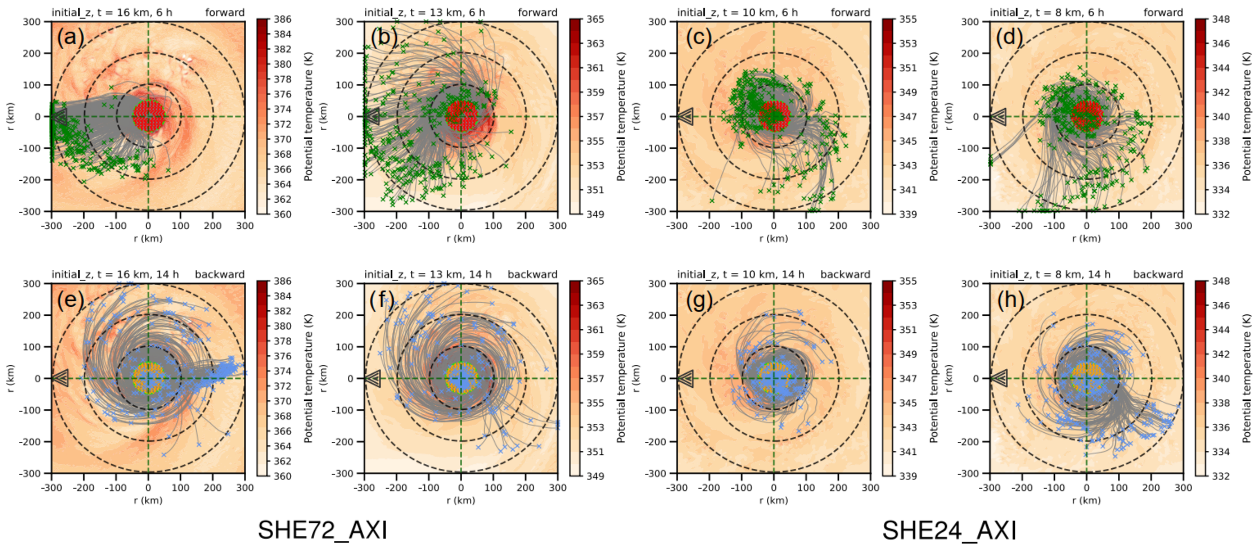

Figure 4. (a, b, e, f) The horizontal distribution of θ (shading; K) at z=16 and 13 km heights after the 6-h simulation with shear, superposed with the following 8-h horizontal trajectories (gray lines) in SHE72_AXI with red (orange) points (in the lime circle) and green (blue) crosses indicating the beginning and ending points of the forward (backward) trajectories, respectively. The start times for the forward and backward trajectories are 6 h and 14 h of shear simulation, and the start levels are 16-km and 13-km heights, respectively. The black arrows indicate the direction of the environmental VWS, and the dashed black circles are plotted every 100 km from the TC center. (c, d, g, h) As in (a, b, e, f) but for SHE24_AXI at the 10-km and 8-km heights, respectively.

The above discussion focuses mainly on the weakening due to the upper-level ventilation associated with the warm-core structure. Since previous studies have also demonstrated the importance of boundary layer ventilation to the TC weakening in environmental VWS (e.g., Gu et al., 2015; Riemer et al., 2010), it is of interest to further examine the boundary-layer ventilation during the early weakening stage of the TC when the upper-level ventilation obviously occurred. We calculated the low-level ventilation, which is the sum of the radial and downdraft ventilations averaged in the boundary layer. The radial ventilation is defined as $\rho u'\theta_e'$ (u'<0) and the downdraft ventilation is defined as $\rho w'\theta_e'$ (w'<0), where ρ is density, u' and w' are asymmetric radial and vertical velocities, and θ_e' is the perturbation equivalent potential temperature from its azimuthal mean. The positive radial ventilation represents the radial eddy flux of anomalously low θ_e air into the inner core, as defined in Tang & Emanuel (2010), and the positive downdraft ventilation represents the downward transport of anomalously low θ_e air into the boundary layer, as discussed in Riemer et al. (2010).

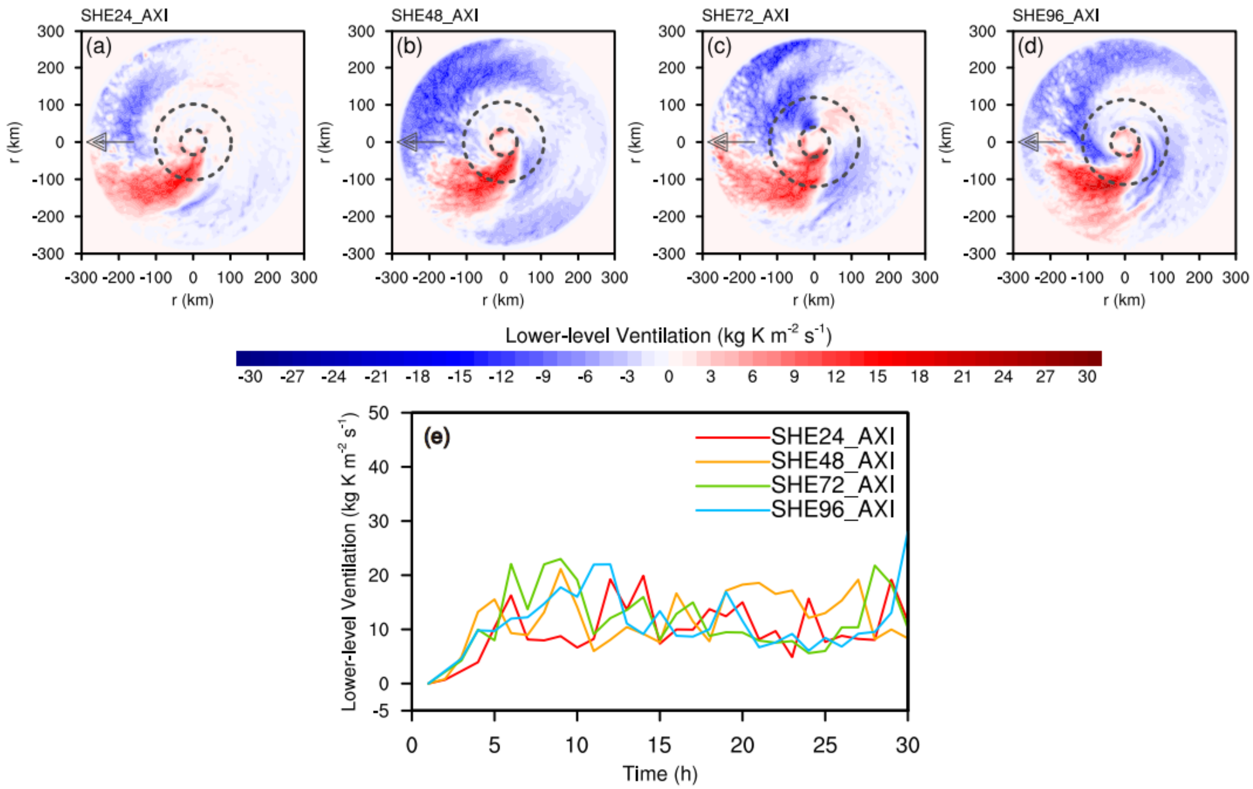

Figure 5. (a-d) Low-level ventilation (kg K m^{-2} s^{-1}) averaged below z=1.5 km in the 24-h period after the VWS was imposed. Red shading means radially inward and vertically downward transport of anomalously low θ_e air. The area within the black dashed big circle indicates the inner core and the small circle nearly indicates the central location of the eyewall. The grey arrows indicate the direction of the environmental VWS; (e) time evolutions of the low-level ventilation (kg K m^{-2} s^{-1}) averaged in the inner core up to 30 h in the shear experiments. The red, orange, green and blue colors represent the VWS experiments with TC vortices after 24, 48, 72, and 96 h of the simulation in CTRL, respectively.

Figures 5a-d show the horizontal distribution of the low-level ventilation averaged within the boundary layer and in the first 24 h after shear was imposed. To quantify these values, we calculated the averaged values within the inner core (3 times the radius of the maximum wind) and found that the averaged low-level ventilations in four shear experiments were 10.03, 12.13, 12.06, 11.42 kg K m^{-2} s^{-1}, respectively, which showed no clear relationship with the early TC intensity change rate. Figure 5e shows the time evolution of low-level ventilation averaged in the inner core during the first 30 h of shear experiments, which does not show any clear relationship with the TC weakening rate. Therefore, we can conclude that the different early TC intensity change rates among the four shear experiments resulted mainly from the upper-level ventilation with little contributions by the low-level ventilation.

4. Conclusions

In this study, idealized numerical experiments were conducted to investigate the dependence of TC intensity change rate in response to an imposed environmental moderate deep-layer VWS on the initial warm-core strength and height during the TC intensifying period on an *f*-plane. Results show that the weakening of the upper-level warm core is the primary factor to the early TC weakening in response to an imposed moderate environmental VWS. The stronger and higher the warm core of the initial TC vortex is, the stronger the upper-level ventilation and thus the larger weakening rate of the upper-level warm core and the TC in response to the imposed moderate VWS. At the early intensifying stage with a weak and lower warm core, the TC intensification is little affected by the imposed moderate VWS because there is almost no significant warm-core ventilation. However, at the later intensifying stage when the warm core becomes stronger and higher, the upper-level warm-core implies relatively strong ventilation, resulting in a great weakening of the upper-level warm core and thus the TC.

Results from the azimuthal mean potential temperature ($\bar{\theta}$) budget reveal that the weakening of the upper-level warm core was largely contributed by the eddy radial advection. Namely, the stronger and higher asymmetric outflow transports the inner-core high θ air outward downshear and downshear-left, as demonstrated by the trajectory analysis, leading to the weakening of the upper-level warm core and thus the TC. In addition, we also show that the magnitudes of the low-level ventilation do not exhibit any clear differences among all shear experiments, suggesting that the different rates of TC intensity change among different shear experiments resulted primarily from the upper-level ventilation in the early response of the TC to the imposed environmental VWS.

Our findings are supported by recent case studies by Rogers et al. (2020) and Stone et al. (2023), who showed that Hurricanes Hermine (2016) and Sally (2020) experienced intensification in their early weak stage (with weak warm core) in the presence of moderate VWS. Our results also support the result of Fu et al. (2019) and Finocchio & Rios-Berrios (2021) who found that the environmental VWS caused the more significant TC weakening at the later intensification stage of the TC in moderate VWS. Although Riemer et al. (2010) found the importance of the low-level ventilation to TC weakening in environmental VWS, their results might be applicable to the environment with VWS over 15 m s^{-1} and a relatively dry mid-troposphere. The findings from this study can help understand why some TCs can develop under the influence of the moderate environmental VWS while some others cannot. The key to the rate of TC intensity change in response to an imposed environmental VWS could be the different warm-core strengths and heights of the initial TC vortices. In addition, we would mention that the upper-level ventilation may be sensitive to the inner-core (warm-core) size of a TC. Namely, a larger TC with a large-sized warm core could have a stronger resilience to an imposed moderate environmental VWS. This can explain why larger TCs weaken less in environmental VWS as found in previous studies (e.g., Wong & Chan, 2004; Bi et al., 2023).

Acknowledgments

The authors acknowledge three anonymous reviewers for their valuable comments that helped to improve the manuscript and thank Prof. Qingqing Li and Prof. Jianfeng Gu for their helpful discussions in early stage of this study. Q. Gao was supported by National Natural Science Foundation of China under grant 41730960 and Y. Wang was supported by NSF grant AGS-1834300.

Open Research

All simulation data that support the findings of this study are publicly available from Gao and Wang (2024).

References

Alland, J. J., Tang, B. H., Corbosiero, K. L., & Bryan, G. H. (2021a). Combined effects of midlevel dry air and vertical wind shear on tropical cyclone development. Part I: Downdraft ventilation. *Journal of the Atmospheric Sciences*, *78*(3), 763–782. https://doi.org/10.1175/JAS-D-20-0054.1

Alland, J. J., Tang, B. H., Corbosiero, K. L., & Bryan, G. H. (2021b). Combined effects of midlevel dry air and vertical wind shear on tropical cyclone development. Part II: Radial ventilation. *Journal of the Atmospheric Sciences*, *78*(3)*,* 783–796. https://doi.org/10.1175/JAS-D-20-0055.1

Bhatia, K. T., & Nolan, D. S. (2013). Relating the skill of tropical cyclone intensity forecasts to the synoptic environment. *Weather Forecasting*, *28*(4), 961–980. https://doi.org/10.1175/WAF-D-12-00110.1

Bi, M.-Y., Wang, R.-F., Li, T., & Ge, X.-Y. (2023). Effects of vertical shear on intensification of tropical cyclones of different initial sizes. *Frontiers in Earth Science*, 11, 1106204. https:/doi.org/10.3389/feart.2023.1106204

Braun, S. A., & Wu, L. (2007). A numerical study of Hurricane Erin (2001). Part II: Shear and the organization of eyewall vertical motion. *Monthly Weather Review*, *135*(4), 1179–1194. https://doi.org/10.1175/MWR3336.1

Chen, X., Gu, J. -F., Zhang, J. A., Marks, F. D., Rogers, R. F., & Cione, J. J. (2021). Boundary layer recovery and precipitation symmetrization preceding rapid intensification of tropical cyclones under Shear. *Journal of the Atmospheric Sciences*, *78*(5), 1523–1544. https://doi.org/10.1175/JAS-D-20-0252.1

Dai, Y. F., Li, Q. -Q., Liu, X. H., & Wang, L. J. (2023). A Lagrangian trajectory analysis of azimuthally asymmetric equivalent potential temperature in the outer core of sheared tropical cyclones. *Advanced in Atmospheric Sciences*, *40*(9), 1689-1706. https://doi:10.1007/s00376-023-2245-0

Dunion, J. P. (2011). Rewriting the climatology of the tropical north Atlantic and Caribbean Sea atmosphere. *Journal of Climate*, *24*(3), 893–908. https://doi.org/10.1175/2010JCLI3496.1

Durden, S. L. (2013). Observed tropical cyclone eye thermal anomaly profiles extending above 300 hPa. *Monthly Weather Review, 141*(2), 4256–4268. https://doi.org/10.1175/MWR-D-13-00021.1

Finocchio, P. M., & Rios-Berrios, R. (2021). The intensity- and size-dependent response of tropical cyclones to increasing vertical wind shear. *Journal of Atmospheric Sciences*, *78*(11), 3673-3609. https://doi:10.1175/JAS-D-21-0126.1

Frank, W. M., & Ritchie, E. A. (2001). Effects of vertical wind shear on the intensity and structure of numerically simulated hurricanes. *Monthly Weather Review*, *129*(9), 2249–2269. https://doi.org/10.1175/1520-0493(2001)129<2249:EOVWSO>2.0.CO;2

Fu, H., Wang, Y., Riemer, M., & Li, Q.-Q. (2019). Effect of unidirectional vertical wind shear on tropical cyclone intensity change – Lower-layer shear versus upper-layer shear. *Journal of Geophysical Research – Atmospheres*, *124*(12)*,* 6265–6282. https://doi.org/10.1029/2019JD030586

Gao, Q., & Wang, Y. (2023). The effect of initial vortex asymmetric structure on tropical cyclone intensity change in response to an imposed environmental vertical wind shear. *Geophysical Research Letters*, *50*(16), e2023GL104222. https://doi.org/10.1029/2023GL104222

Gao, Q., & Wang, Y. (2024). Simulation data for "Dependence of tropical cyclone weakening rate in response to an imposed moderate environmental vertical wind shear on the warm-core strength and height of the initial vortex." [Dataset]. Dryad. https://doi.org/doi:10.5061/dryad.xgxd254nq

Gray, W. M. (1968). Global view of the origin of tropical disturbances and storms. *Monthly Weather Review*, *96*(10), 669–700. https://doi.org/10.1175/1520-0493(1968)096<0669:GVOTOO>2.0.CO;2

Gu, J.-F., Tan, Z.-M., & Qiu, X. (2015). Effects of vertical wind shear on inner-core thermodynamics of an idealized simulated tropical cyclone. *Journal of Atmospheric Sciences*, *72*(2), 511–530. https://doi.org/10.1175/JAS-D-14-0050.1

Gu, J.-F., Tan, Z.-M., & Qiu, X. (2018). The evolution of vortex tilt and vertical motion of tropical cyclones in directional shear flows. *Journal of the Atmospheric Sciences*, *75*(10), 3565–3578. https://doi.org/10.1175/JAS-D-18-0024.1

Gu, J.-F., Tan, Z.-M., & Qiu, X. (2019). Intensification variability of tropical cyclones in directional shear flows: vortex tilt–convection coupling. *Journal of the Atmospheric Sciences*, *76*(6), 1827–1844. https://doi.org/10.1175/JAS-D-18-0282.1

Hendricks, E. A., Peng, M. S., Fu, B., & Li, T. (2010). Quantifying environmental control on tropical cyclone intensity change. *Monthly Weather Review*, *138*(8), 3243–3271. https://doi.org/10.1175/2010MWR3185.1

Liu, H.-Y., Wang, Y., & Gu, J.-F. (2021). Intensity change of binary tropical cyclones (TCs) in idealized numerical simulations: Two initially identical mature TCs. *Journal of the Atmospheric Sciences*, *78*(4), 1001–1020. https://doi.org/10.1175/JAS-D-20-0116.1

Liu, X. H., Li, Q. -Q. & Dai, Y. F. (2022). Stronger vertical shear leads to earlier secondary eyewall formation in idealized numerical simulations. *Geophysical Research Letters*, *49*(10), e2022GL098093. https://doi.org/10.1029/2022GL098093

Miller, W., & Zhang, D.-L. (2019). A three-dimensional trajectory model with advection correction for tropical cyclones: Algorithm description and tests for accuracy. *Monthly Weather Review*, *147*(9), 3145-3167. https://doi.org/10.1175/MWR-D-18-0434.1

Molinari, J., Dodge, P., Vollaro, D., Corbosiero, K. L., & Marks, F. (2006). Mesoscale aspects of the downshear reformation of a tropical cyclone. *Journal of the Atmospheric Sciences*, *63*(1), 341–354. https://doi.org/10.1175/JAS3591.1

Nguyen, L. T., & Molinari, J. (2012). Rapid intensification of a sheared, fast-moving hurricane over the Gulf Stream. *Monthly Weather Review*, *140*(10), 3361–3378. https://doi.org/10.1175/MWR-D-11-00293.1

Nguyen, L. T., Rogers, R., Zawislak, J., & Zhang, J. A. (2019). Assessing the influence of convective downdrafts and surface enthalpy fluxes on tropical cyclone intensity change in moderate vertical wind shear. *Monthly Weather Review*, *147*(10), 3519–3534. https://doi. org/10.1175/MWR-D-18-0461.1

Ohno, T., Satoh, M., & Yamada, Y. (2016). Warm cores, eyewall slopes, and intensities of tropical cyclones simulated by a 7-km-mesh global nonhydrostatic model. *Journal of the Atmospheric Sciences*, *73*(11), 4289–

4309. https://doi.org/10.1175/JAS-D-15-0318.1

Onderlinde, M. J., & Nolan, D. S. (2017). The tropical cyclone response to changing wind shear using the method of time-varying point-downscaling. *Journal of Advances in Modeling Earth Systems*, *9*(2), 908–931. https://doi. org/10.1002/2016MS000796

Reasor, P. D., & Eastin, M. D. (2012). Rapidly intensifying Hurricane Guillermo (1997). Part II: Resilience in shear. *Monthly Weather Review*, *140*(2), 425–444. https://doi.org/10.1175/MWR-D-11-00080.1

Reasor, P. D., Rogers, R., & Lorsolo, S. (2013). Environmental flow impacts on tropical cyclone structure diagnosed from airborne Doppler radar composites. *Monthly Weather Review*, *141*(9), 2949–2969. https://doi.org/10.1175/MWR-D-12-00334.1

Riemer, M., & Montgomery, M. T. (2011). Simple kinematic models for the environmental interaction of tropical cyclones in vertical wind shear. *Atmospheric Chemistry and Physics*, *11*(17), 9395–9414. https://doi.org/10.5194/acp-11-9395-2011

Riemer, M., Montgomery, M. T., & Nicholls, M. E. (2010). A new paradigm for intensity modification of tropical cyclones: Thermodynamic impact of vertical wind shear on the inflow layer. *Atmospheric Chemistry and Physics*, *10*(7), 3163–3188. https://doi.org/10.5194/acpd-9-10711-2009

Rios-Berrios, R. (2020). Impacts of radiation and cold pools on the intensity and vortex tilt of weak tropical cyclones interacting with vertical wind shear. *Journal of the Atmospheric Sciences*, *77*(2), 669–689. https://doi.org/10.1175/JAS-D-19-0159.1

Rios-Berrios, R., Torn, R. D., & Davis, C. A. (2016). An ensemble approach to investigate tropical cyclone intensification in sheared environments. Part I: Katia (2011). *Journal of the Atmospheric Sciences*, *73*(1), 71–93. https://doi.org/10.1175/JAS-D-15-0052.1

Rogers, R. F., Reasor, P. D., Zawislak, J. A., & Nguyen, L. T. (2020). Precipitation processes and vortex alignment during the intensification of a weak tropical cyclone in moderate vertical shear. *Monthly Weather Review*, *148*(5), 1899–1929. https://doi.org/10.1175/MWR-D-19-0315.1

Rotunno, R., & Emanuel, K. A. (1987). An air-sea interaction theory for tropical cyclones. Part II: Evolutionary study using a nonhydrostatic axisymmetric numerical model. *Journal of the Atmospheric Sciences*, *44*(3), 542–561. https://doi.org/10.1175/1520-0469(1987)044<0542:AAITFT>2.0.CO;2

Ryglicki, D. R., Doyle, J. D., Hodyss, D., Cossuth, J. H., Jin, Y., Viner, K. C., & Schmidt, J. M. (2019). The unexpected rapid intensification of tropical cyclones in moderate vertical wind shear. Part III: Outflow–environment interaction. *Monthly Weather Review*, *147*(8), 2919–2940. https://doi.org/10.1175/MWR-D-18-0370.1

Shi, D. L., & Chen, G. H. (2021). Double warm-core structure and potential vorticity diagnosis during the rapid intensification of Supertyphoon Lekima (2019). *Journal of the Atmospheric Sciences*, *78*(8), 2471-2492. https://doi.org/10.1175/JAS-D-20-0383.1

Skamarock, W. C., Klemp, J. B., Dudhia, J., Gill, D. O., Barker, D. M., Duda, M. G., Huang, X. Y., Wang, W., & Powers, J. G. (2008). A description of the advanced research WRF version 3. *NCAR Tech. Note NCAR/TN-*

4751STR, *113*. [Available online at http://www.mmm.ucar.edu/wrf/users/docs/ arw_v3_bw.pdf.]

Stern, D. P., & Zhang, F. (2013). How does the eye warm? Part I: A potential temperature budget analysis of an idealized tropical cyclone. *Journal of the Atmospheric Sciences*, *70*(1), 73–90. https://doi.org/10.1175/JAS-D-11-0329.1

Stone, Z., Alvey, G. R., Dunion, J. P., Fischer, M. S., Raymond, D. J., Rogers, R. F., Sentic, S., & Zawislak, J. (2023). Thermodynamic contribution to vortex alignment and rapid intensification of Hurricane Sally (2020). *Monthly Weather Review, 151*(4), 931–951. https://doi.org/10.1175/MWR-D-22-0201.1

Tang, B., & Emanuel, K. (2010). Midlevel ventilation's constraint on tropical cyclone intensity. *Journal of the Atmospheric Sciences*, *67*(6), 1817–1830. https://doi.org/10.1175/2010JAS3318.1

Tang, B., & Emanuel, K. (2012). Sensitivity of tropical cyclone intensity to ventilation in an axisymmetric model. *Journal of the Atmospheric Sciences*, *69*(8), 2394–2413. https://doi.org/10.1175/JAS-D-11-0232.1

Wang, H., Wang, Y., Xu, J., & Duan, Y. (2019). Evolution of the warm-core structure during the eyewall replacement cycle in a numerically simulated tropical cyclone. *Journal of the Atmospheric Sciences*, *76*(8), 2559–2573. https://doi.org/10.1175/JAS-D-19-0017.1

Wang. Y., & Holland, G. J. (1996). Tropical cyclone motion and evolution in vertical shear. *Journal of the Atmospheric Sciences*, *53*(22), 3313–3332. https://doi.org/10.1175/1520-0469(1996)053,3313:TCMAEI.2.0.CO;2

Wang. Y., Rao, Y., Tan, Z.-M., & Schönemann, D. (2015). A statistical analysis of the effects of vertical wind shear on tropical cyclone intensity change over the western North Pacific. *Monthly Weather Review*, *143*(9), 3434–3453. https://doi.org/10.1175/MWR-D-15-0049.1

Wong, M. L. M., & Chan, J. C. L. (2004). Tropical cyclone intensity in vertical wind shear. *Journal of the Atmospheric Sciences*, *61*(15), 1859–1876. https://doi.org/10.1175/1520-0469(2004)061<1859:TCIIVW>2.0.CO;2

Xi, D., Chu, K., Tan, Z.-M., Gu, J.-F., Shen, W., Zhang, Y., & Tang, J. (2021). Characteristics of warm cores of tropical cyclones in a 25-km-mesh regional climate simulation over CORDEX East Asia domain. *Climate Dynamics*, *57*, 2375–2389. https://doi.org/10.1007/s00382-021-05806-9

Xu, Y.-M., & Wang, Y. (2013). On the initial development of asymmetric vertical motion and horizontal relative flow in a mature tropical cyclone embedded in environmental vertical shear. *Journal of the Atmospheric Sciences*, *70*(11), 3471–3491. https://doi.org/10.1175/JAS-D-12-0335.1

Zehr, R. Branch, M., R., & Collins, F. (1992). Tropical cyclogenesis in the western North Pacific. *NOAA Technical Report NESDIS, 46*. https://repository.library.noaa.gov/view/noaa/13116/noaa_13116_DS1.pdf

Zeng, Z., Wang, Y. & Chen, L.-S. (2010). A statistical analysis of vertical shear effect on tropical cyclone intensity change in the north Atlantic: Vertical shear effect on TC intensity. *Geophysical Research Letters*, *37*(2), L02802. https://doi.org/10.1029/2009GL041788